Submitted: 30 October, 2023 Accepted: 27 December, 2023 Published: 30 July, 2024 DOI:10.22514/jomh.2024.107

ORIGINAL RESEARCH

JOMH Journal of Men's Health

A novel prognosis and drug-susceptibility predictor based inflammatory-related genes signature in prostate cancer

Mao Wang[1], Hao Dong[1], Zhi-Yao He[1,*]

[1]Department of Pharmacy, West China Hospital, Sichuan University, 610041 Chengdu, Sichuan, China

***Correspondence**
zhiyaohe@scu.edu.cn
(Zhi-Yao He)

Abstract

Prostate cancer (PCa) is a widespread global health concern affecting males. Numerous investigations have shown the substantial implications of inflammation to PCa progression. To evaluate the predictive capacity of inflammatory-related genes (IRGs) in PCa, we conducted univariate Cox regression analysis and the Least Absolute Shrinkage and Selector Operation (LASSO) regression to formulate a prognostic model based on IRG expression. The training dataset comprised The Cancer Genome Atlas (TCGA) cohort, with validation performed using the cBioPortal cohort. Subsequently, an overall survival (OS) prediction was performed using a nomogram within the TCGA-PCa cohort, and we explored the association between the risk model and various factors such as immune cell infiltration, immune-related pathway functionality, tumor microenvironment characteristics, cancer stem cell scores and drug sensitivity. A comprehensive selection of 17 IRGs was identified to establish this prognostic risk model, where individuals with elevated risk scores exhibited unfavorable prognosis. The genomic nomogram, constructed based on these central IRGs, demonstrated remarkable accuracy in predicting PCa prognosis. Evaluation of tumor-infiltrating immune cells and immune-related pathways suggested that high-risk groups may manifest an immune-active phenotype. Moreover, there was a significant correlation between the expression levels of IRGs and tumor cell sensitivity to chemotherapeutic drugs. In conclusion, these findings indicate that an IRG-based risk model associated with inflammation can effectively predict PCa prognosis, presenting a promising strategy for further investigation.

Keywords

Prostate cancer; TCGA; Inflammatory-related genes; Immune; LASSO regression

1. Introduction

Prostate cancer (PCa) is the most prevalent malignancy in males, accounting for approximately 20% of all cancer cases and contributing to 6.8% of male cancer-related deaths globally [1]. In the United States, it has been observed that 14% to 24% of individuals diagnosed with PCa are classified as high-risk patients, even after undergoing prostate-specific antigen (PSA) screening [2–5]. High-risk prostate cancer is defined by a preoperative PSA level exceeding 20 ng/mL, a Gleason score of 8 or higher, or a clinical stage of T2c or greater [6, 7]. Patients diagnosed with PCa exhibiting a high-risk profile display significant diversity, leading to uncertainty regarding the most appropriate treatment strategy [8, 9]. Despite the availability of various treatment options, including radical prostatectomy, radiation therapy and hormone therapy, either as monotherapies or in combination, the recurrence rate remains substantially elevated regardless of the chosen treatment modality [10, 11].

The comprehensive identification of the causal factors responsible for the initiation and progression of PCa remains an ongoing area of research. PCa prominently displays an inflammatory component, recognized as a fundamental hallmark of cancer influencing various stages of carcinogenesis and tumor advancement [12]. Likewise, there is evidence indicating a connection between prostatitis, a frequently encountered condition characterized by acute or chronic prostate infection, and an increased susceptibility to PCa [13, 14]. The prevailing hypothesis suggests that persistent inflammation within the prostate gland stimulates the production of inflammatory cytokines and reactive oxygen species, promoting increased cellular proliferation and potentially facilitating carcinogenesis [15–18].

In PCa, the presence of inflammatory alterations is characterized by an increased infiltration of inflammatory cells and the release of proinflammatory cytokines, which contributes to the activation of numerous signaling pathways associated with PCa progression [19, 20]. Although previous research

has established a link between inflammation and the development and metastasis of PCa, it remains uncertain whether inflammation and its associated genes can impact PCa prognosis. Therefore, it is essential to identify inflammatory-related genes (IRGs) associated with PCa to provide a scientifically grounded prognosis.

The primary objective of this study was to investigate the influence of inflammation and its associated genes on the prognosis of PCa patients. We conducted an analysis involving 17 IRGs to establish a risk signature by integrating high-throughput data for predicting PCa patient prognosis, and the findings demonstrate that our prognostic model achieves a high level of accuracy in predicting PCa prognosis and could serve as a novel and valuable reference point for the clinical prediction and management of PCa.

2. Methods

2.1 Data acquisition

In this study, we accessed publicly available data, including transcriptome profiling (RNA-seq) data, clinical information, immune subtypes, and stemness scores derived from DNA-methylation (DNAss) and mRNA (RNAss) analyses, encompassing 475 PCa samples and 52 para-cancerous samples. These datasets were retrieved from The Cancer Genome Atlas (TCGA) database, accessible at https://portal.gdc.cancer.gov/. For external validation, we utilized an additional cohort comprising 268 samples from the cBioPortal cohort [21, 22]. To identify relevant IRGs, we curated a set of 200 genes from the "HALLMARK_INFLAMMATORY_RESPO-NSE" gene set, sourced from the GSEA database, available at http://www.gsea-msigdb.org/ [23].

2.2 Screening and visualizing hub IRGs

Univariate Cox hazards regression analysis was performed on the acquired prognostic IRGs and identified potential hub IRGs using the "survival" R package, and the least absolute shrinkage and selection operator (LASSO) regression was used to refine this set of IRGs. To identify the common genes of interest, a Venn diagram was constructed. The visualization of hub IRGs was accomplished through a heatmap generated with the "pheatmap" R package. Furthermore, we generated a forest plot using the "forest plot" R package to present the hazard ratio (HR), 95% confidence interval (CI), and *p*-value for each variable.

2.3 Construction and validation of a risk assessment model

Subsequently, we established the risk assessment model through multivariate Cox regression analysis. Patient risk scores were calculated using the following formula: risk score = $\beta 1 \times 1 + \beta 2 \times 2 + \ldots + \beta \mathrm{i} \times \mathrm{i}$, where $\times$ i represents the expression level of genes, and βi signifies the corresponding coefficient obtained from the multivariate Cox regression analysis. Patients diagnosed with PCa in both the TCGA and cBioPortal cohorts were categorized into either the low-risk or high-risk group based on their risk scores, which were determined using the median value. To assess the prognostic distinction between these two groups, we conducted Kaplan-Meier survival analysis. Furthermore, we evaluated the predictive performance by calculating the area under the time-dependent receiver operating characteristic (ROC) curve (AUC) using the "time ROC" R package.

2.4 Prognostic nomogram and clinical characteristics value evaluation

To explore the relationship between IRGs and PCa patients, we developed a genomic nomogram using the identified IRGs to predict the 1-, 3- and 5-year survival probabilities for each patient with the "rms" R package. Additionally, we performed univariate and multivariate Cox Hazards regression analyses to determine the significance of the risk score, along with other potential prognostic markers such as age and TNM (Tumor node metastasis) classification; T: Tumor; N: Lymph Node; M: Metastasis), in predicting the prognosis of PCa patients.

2.5 Investigations of the tumor microenvironment (TME), function enrichment analysis, DNA methylation pattern and mRNA expression

Gene Set Enrichment Analysis (GSEA) was conducted to examine differences in enrichment between the high-risk and low-risk groups concerning the activity of immune-related pathways. To assess and quantify variations in immune cell activity and immune function between these groups, we utilized single-sample gene set enrichment analysis (ssGSEA) with the "GSEABase" and "GSVA" R packages [24, 25]. Furthermore, we employed the "ESTIMATE" R package to compute the immune score, stromal score and ESTIMATE score [26].

2.6 Drug sensitivity analysis

To investigate the potential correlation between IRGs and the sensitivity of chemotherapeutic drugs, we acquired the NCI60 drug response data using the CellMiner tool at https://discover.nci.nih.gov/cellminer. This dataset included information from 60 distinct cell lines representing 9 different types of malignancies [27]. Then, Pearson correlation analysis was performed to assess the relationship between IRGs and the efficacy of chemotherapy drugs that have received approval from the Food and Drug Administration (FDA) or are currently undergoing clinical trials.

2.7 Statistical analysis

All statistical analyses were conducted using R version 4.0.3 (https://www.R-project.org/). To evaluate the association between risk scores and cancer stemness scores, Spearman's test was employed. Pearson's test was utilized to assess the correlation between gene expression and drug sensitivity. Additionally, the Wilcoxon rank-sum test, a commonly used nonparametric statistical test for comparing two groups, was applied. A significance level of $p < 0.05$ was considered statistically significant.

TABLE 1. Univariate Cox regression analysis of 44 identified IRGs.

Genes	HR	HR.95L	HR.95H	Hazard.Ratio	*p*.value
ADRM1	3.020	1.585	5.755	3.020 (1.585–5.755)	<0.001
APLNR	1.386	1.138	1.687	1.386 (1.138–1.687)	0.001
BDKRB1	2.560	1.187	5.520	2.560 (1.187–5.520)	0.016
BST2	1.244	1.038	1.490	1.244 (1.038–1.490)	0.018
BTG2	0.819	0.674	0.995	0.819 (0.674–0.995)	0.044
C3AR1	1.434	1.105	1.861	1.434 (1.105–1.861)	0.007
C5AR1	1.364	1.080	1.723	1.364 (1.080–1.723)	0.009
CCL17	1.279	1.056	1.549	1.279 (1.056–1.549)	0.012
CCL24	1.331	1.091	1.624	1.331 (1.091–1.624)	0.005
CCRL2	1.530	1.005	2.331	1.530 (1.005–2.331)	0.047
CD14	1.410	1.097	1.814	1.410 (1.097–1.814)	0.007
CLEC5A	1.852	1.085	3.161	1.852 (1.085–3.161)	0.024
CSF3R	1.668	1.196	2.326	1.668 (1.196–2.326)	0.003
DCBLD2	0.614	0.458	0.822	0.614 (0.458–0.822)	0.001
ADGRE1	1.987	1.097	3.599	1.987 (1.097–3.599)	0.024
FZD5	0.731	0.585	0.913	0.731 (0.585–0.913)	0.006
GABBR1	1.530	1.155	2.026	1.530 (1.155–2.026)	0.003
GPR132	1.392	1.044	1.856	1.392 (1.044–1.856)	0.024
IL10RA	1.310	1.034	1.659	1.310 (1.034–1.659)	0.025
IL18	1.315	1.022	1.691	1.315 (1.022–1.691)	0.033
IL1R1	0.777	0.615	0.982	0.777 (0.615–0.982)	0.035
INHBA	1.241	1.038	1.484	1.241 (1.038–1.484)	0.018
IRF7	1.743	1.293	2.350	1.743 (1.293–2.350)	<0.001
KCNJ2	1.408	1.063	1.865	1.408 (1.063–1.865)	0.017
LTA	1.531	1.107	2.116	1.531 (1.107–2.116)	0.010
LY6E	1.322	1.030	1.696	1.322 (1.030–1.696)	0.029
MEFV	1.692	1.021	2.805	1.692 (1.021–2.805)	0.041
MSR1	1.424	1.110	1.828	1.424 (1.110–1.828)	0.005
NDP	0.688	0.545	0.869	0.688 (0.545–0.869)	0.002
OPRK1	1.204	1.037	1.396	1.204 (1.037–1.396)	0.014
OSM	1.382	1.109	1.722	1.382 (1.109–1.722)	0.004
PCDH7	0.760	0.613	0.943	0.760 (0.613–0.943)	0.013
PIK3R5	1.629	1.197	2.218	1.629 (1.197–2.218)	0.002
PTAFR	1.325	1.011	1.736	1.325 (1.011–1.736)	0.041
PTGIR	2.623	1.723	3.994	2.623 (1.723–3.994)	<0.001
SCARF1	2.205	1.549	3.139	2.205 (1.549–3.139)	<0.001
SCN1B	1.440	1.031	2.013	1.440 (1.031–2.013)	0.032
SEMA4D	1.772	1.081	2.905	1.772 (1.081–2.905)	0.023
SLC7A1	0.752	0.594	0.952	0.752 (0.594–0.952)	0.018
SPHK1	1.559	1.183	2.053	1.559 (1.183–2.053)	0.002
SRI	1.872	1.135	3.089	1.872 (1.135–3.089)	0.014
STAB1	1.517	1.168	1.969	1.517 (1.168–1.969)	0.002
TNFAIP6	1.452	1.057	1.995	1.452 (1.057–1.995)	0.021
TNFRSF1B	1.292	1.004	1.661	1.292 (1.004–1.661)	0.046

HR: hazard ratio; HR.95L&H: HR 95% confidence interval; L: lower; H: higher.

3. Results

3.1 Identification of prognostic IRGs

Recognizing the significant influence of the inflammatory response on the development and progression of PCa, we compiled a dataset of human inflammatory response genes from the GSEA database, comprising 200 genes referred to as IRGs. To comprehensively understand the relevance of these genes in PCa, we initially conducted a univariate Cox proportional hazards regression analysis, which revealed 44 IRGs significantly associated with overall survival ($p < 0.05$) (Table 1). Subsequently, we applied LASSO regression analysis to the IRGs, utilizing 10-fold cross-validation to identify optimal tuning parameter values. As shown in Fig. 1A, all coefficients retained non-zero values, and 22 IRGs were stable (Fig. 1B). Then, a total of 17 IRGs were identified as common factors, represented in the Venn diagram (Fig. 1C), and their expression patterns of these 17 IRGs in PCa are shown through a heatmap (Fig. 1D).

3.2 Construction and validation of a risk assessment model in PCa

Next, all the factors derived from the LASSO-Cox regression analysis were included in the multivariate Cox regression analysis (Fig. 1E), based on which a model was established involving 17 IRGs, and a risk score formula was derived as follows: Risk score = Exp (BTG2) × (−0.3188) + Exp (C3AR1) × (0.6855) + Exp (CCL24) × (0.3293) + Exp (CCRL2) × (−1.5837) + Exp (CD14) × (0.3979) + Exp (CLEC5A) × (−0.7633) + Exp (DCBLD2) × (−0.7625) + Exp (GABBR1) × (0.2648) + Exp (KCNJ2) × (0.3135) + Exp (OPRK1) × (0.2719) + Exp (OSM) × (0.5280) + Exp (SCARF1) × (0.8879) + Exp (SCN1B) × (0.5578) + Exp (SEMA4D) × (0.5921) + Exp (SLC7A1) × (−0.3884) + Exp (SPHK1) × (0.5419) + Exp (TNFRSF1B) × (−0.6780) (Table 2). The correlations among these 17 IRGs are shown in Fig. 1F. Subsequently, a nomogram was constructed using these 17 IRGs to predict the 1-, 3- and 5-year survival of PCa patients (Fig. 2A). The cumulative score of each gene was used to calculate the total score, and vertical lines were drawn downwards at the corresponding positions on the total score axis to determine the relative survival rates at 1-, 3- and 5-year intervals. Based on the calculated median risk score, patients were categorized into two groups: the low-risk and high-risk groups. Kaplan-Meier survival curves demonstrated a statistically significant difference between the two cohorts, indicating that those with high-risk scores had a less favorable prognosis compared to those with low-risk scores (Fig. 2B). Subsequently, a time-dependent ROC analysis was conducted to assess the prognostic performance of the IRGs. The AUC for the prognostic model at 1-, 3- and 5-year intervals were determined to be 0.856, 0.764 and 0.828, respectively (Fig. 2C). To validate the prognostic power of the IRGs, an external validation cohort from the cBioPortal dataset was utilized. Consistently, patients classified as high-risk exhibited significantly shorter overall survival compared to those classified as low-risk (Fig. 2D). The AUC values for 1-, 3- and 5-year intervals were 0.756, 0.768 and 0.787, respectively (Fig. 2E). Additionally, TCGA-PCa patients were divided into high-risk and low-risk groups based on the median risk score, which served as the threshold (Fig. 2F). A high-risk score was associated with an increased likelihood of mortality, as evident from the distribution of IRG risk scores and patient survival status (Fig. 2G). These results suggest that the risk score obtained from these 17 IRGs demonstrates a high degree of accuracy and substantial predictive value for assessing the overall survival of PCa patients.

TABLE 2. Multivariate Cox regression analysis of the 17 significant IRGs.

Genes	Coefficients	HR	HR.95L	HR.95H	*p*.value
BTG2	−0.3188	0.7270	0.5390	0.9806	0.0368
C3AR1	0.6855	1.9848	1.1256	3.5000	0.0178
CCL24	0.3293	1.3899	1.1004	1.7557	0.0057
CCRL2	−1.5837	0.2052	0.0685	0.6152	0.0047
CD14	0.3979	1.4887	0.8616	2.5723	0.0539
CLEC5A	−0.7633	0.4661	0.2059	1.0553	0.0671
DCBLD2	−0.7625	0.4665	0.2940	0.7401	0.0012
GABBR1	0.2648	1.3032	0.9392	1.8083	0.0830
KCNJ2	0.3135	1.3682	0.9242	2.0256	0.0873
OPRK1	0.2719	1.3124	1.1130	1.5477	0.0012
OSM	0.5280	1.6955	1.1840	2.4280	0.0040
SCARF1	0.8879	2.4300	1.3428	4.3973	0.0033
SCN1B	0.5578	1.7468	1.2150	2.5113	0.0026
SEMA4D	0.5921	1.8079	0.9289	3.5184	0.0813
SLC7A1	−0.3884	0.6781	0.4905	0.9376	0.0188
SPHK1	0.5419	1.7193	1.0435	2.8326	0.0334

HR: hazard ratio; HR.95L&H: HR 95% confidence interval; L: lower; H: higher.

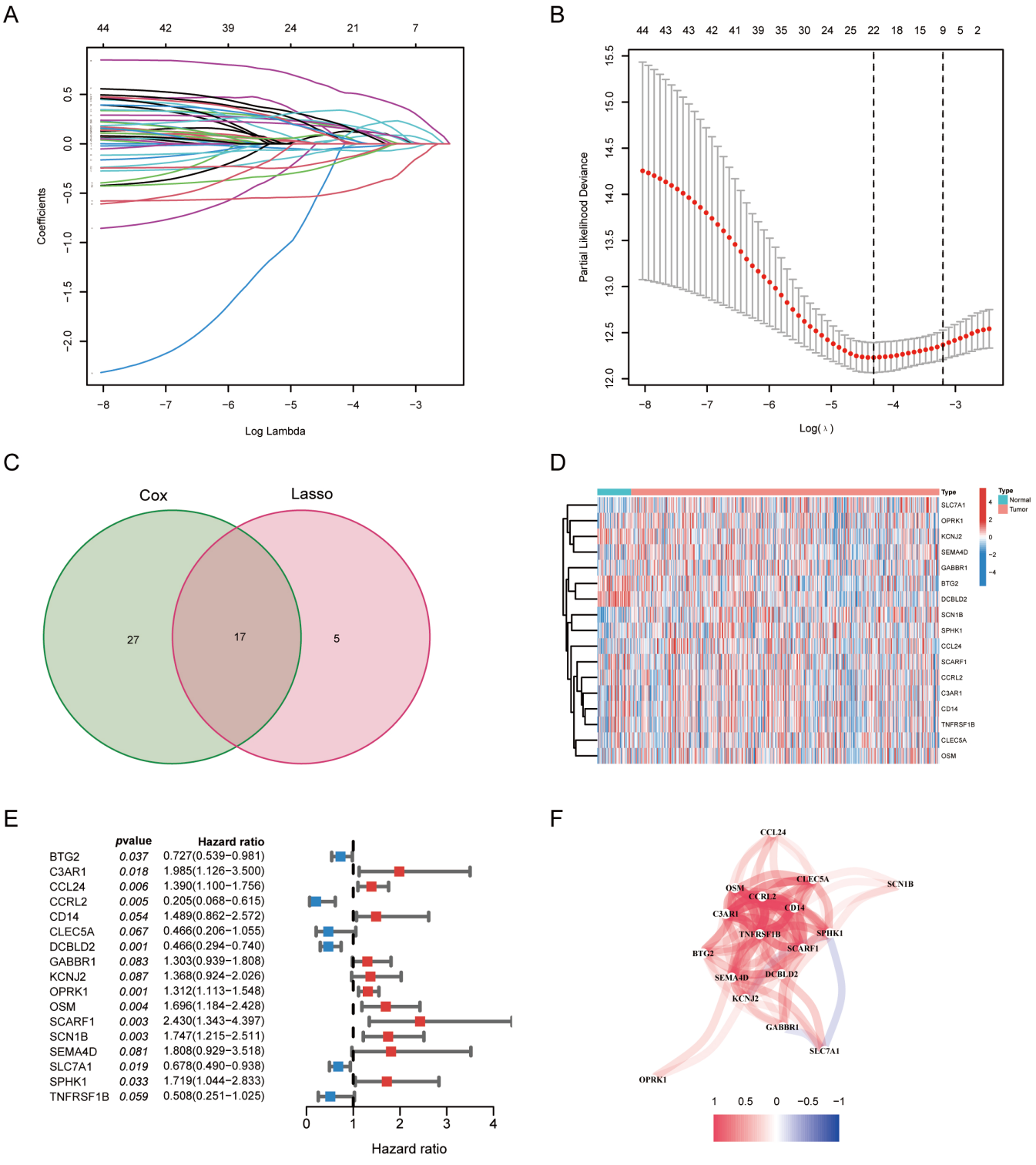

FIGURE 1. Prognostic inflammatory-related gene identification process in prostate cancer. (A,B) Key inflammatory-related genes were selected using LASSO regression analysis. (C) A Venn plot highlights the 17 common prognostic genes associated with inflammatory responses. (D) The heatmap displays the expression of these 17 genes in PCa and normal tissues. (E) A forest plot shows hazard ratios for the 17 prognostic genes, forming the basis for a prognostic model. (F) The correlation plot of signature genes, with red indicating a positive connection and blue indicating a negative association. LASSO: Least Absolute Shrinkage and Selector Operation; PCa: prostate cancer.

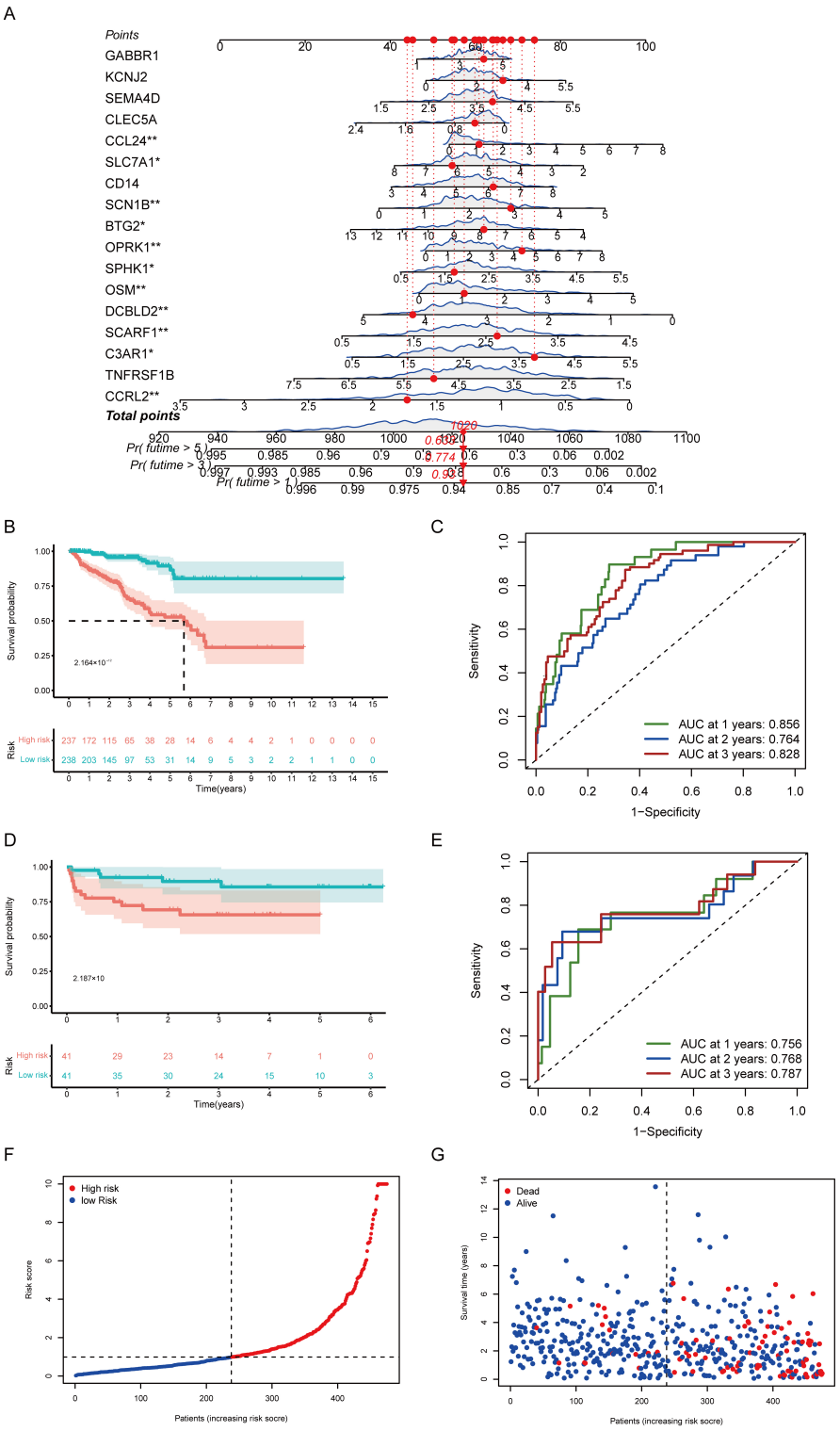

F I G U R E 2. Construction and evaluation of the prognostic model using hub IRGs. (A) A nomogram designed for predicting 1-, 3- and 5-year OS of PCa patients. Vertical lines extend upward to determine values for each variable. The total score is obtained by summing individual variable values, and the anticipated likelihood of OS is determined by extending a vertical line downward from the Total Points axis. (B) Kaplan-Meier curves illustrating the outcomes of low- and high-risk groups in TCGA. (C) Kaplan-Meier curves showing the outcomes of low- and high-risk groups in the cBioPortal cohorts. (D) ROC curves assessing the predictive ability of the risk score for 1-, 3- and 5-year OS in TCGA. (E) ROC curves assessing the predictive ability of the risk score for 1-, 3- and 5-year OS in the cBioPortal cohorts. (F) PCa patients categorized into high- and low-risk groups based on the risk score. (G) Distribution of IRG risk scores and patient survival status. OS: overall survival; PCa: prostate cancer; TCGA: The Cancer Genome Atlas; ROC: receiver operating characteristic; IRG: inflammatory-related genes.

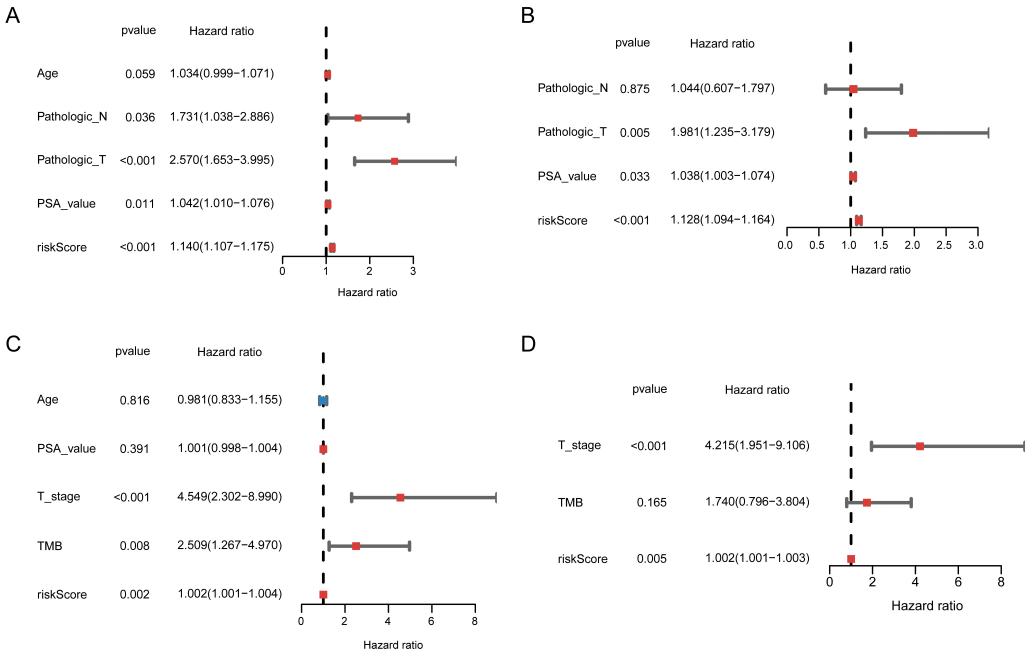

FIGURE 3. Univariate and multivariate Cox regression analyses of the study cohort. (A,B) Univariate and multivariate Cox regression analyses for the TCGA dataset, assessing the impact of various clinicopathological factors and the risk score on prognosis. (C,D) Univariate and multivariate Cox regression analyses for the cBioPortal dataset, evaluating the influence of different clinicopathologic factors and the risk score on prognosis. PSA: prostate-specific antigen; TMB: tumor mutation burden.

3.3 Independent prognostic value of the IRG risk score

We included the risk score and clinical factors in both univariate and multivariate analyses to assess the potential of the IRGs as independent predictors. In the TCGA population, pathological (T) stage, PSA value and risk score were identified as having a significant association with overall survival (OS) based on both univariate and multivariate Cox regression models (Fig. 3A,B). In the univariate analysis ($p < 0.001$), the hazard ratio (HR) for the risk score was 1.140 with a 95% confidence interval (CI) of 1.107–1.175. In the multivariate analysis ($p < 0.001$), the HR for the risk score was 1.128 with a 95% CI of 1.094–1.164. Similarly, in the cBioPortal cohort, univariate and multivariate Cox regression analyses revealed a significant correlation between OS and T stage as well as the risk score (Fig. 3C,D). In the univariate analysis ($p = 0.002$), the HR for the risk score was 1.002 with a 95% CI of 1.001–1.004. In the multivariate analysis ($p = 0.005$), the HR for the risk score was 1.002 with a 95% CI of 1.001–1.003. Collectively, these findings provide strong evidence that the IRG risk score serves as a valuable independent prognostic factor for PCa.

3.4 Tumor microenvironment assessment using the IRG risk score

We used single-sample gene set enrichment analysis (ssGSEA) to quantify 16 immune cell subsets and 13 immune-related functions and evaluate the potential of the IRG risk score in assessing immunological features and elucidating the relationship between the risk score and overall immune status. The analysis of immune cell infiltration revealed a significant positive correlation between the risk score of IRGs and the abundance of various immune infiltrating cells, including tumor-infiltrating lymphocytes (TIL), CD8+ (cluster of differentiation 8) T cells, dendritic cells (DCs), macrophages, plasmacytoid dendritic cells (pDCs), and T helper cells (Fig. 4A). Furthermore, the analysis of immune-related pathways indicated that immunological responses were significantly more pronounced in the high-risk group compared to the low-risk group (Fig. 4B). We also examined the immunophenotyping distribution of different tumor sample types in the TCGA database, revealing risk scores for four distinct immune types (Fig. 4C). To gain a deeper understanding of the underlying functionality of IRGs and their associated signal transduction pathways, we conducted an extensive investigation using Gene Set Enrichment Analysis (GSEA). The results demonstrated significant differences in pathway enrichment between the low-risk and high-risk groups (Fig. 4D). Notably, the high-risk group exhibited positive associations with immune pathways such as cytolytic activity, HLA (human leukocyte antigen), MHC (major histocompatibility complex) class I, and others. These findings suggest that PCa patients with high-risk scores may be more responsive to immunotherapy due to their heightened immune regulation. This insight may offer a new perspective to enhance the effectiveness of immunotherapy in the context of PCa treatment.

Considering the TME and the presence of stromal cells and immune cells play significant roles in cancer, we conducted a correlation analysis to explore the relationship between the risk score and the TME, aiming to better understand the impact of TME on PCa patients. The results reveal a significant positive correlation between the risk score and the presence

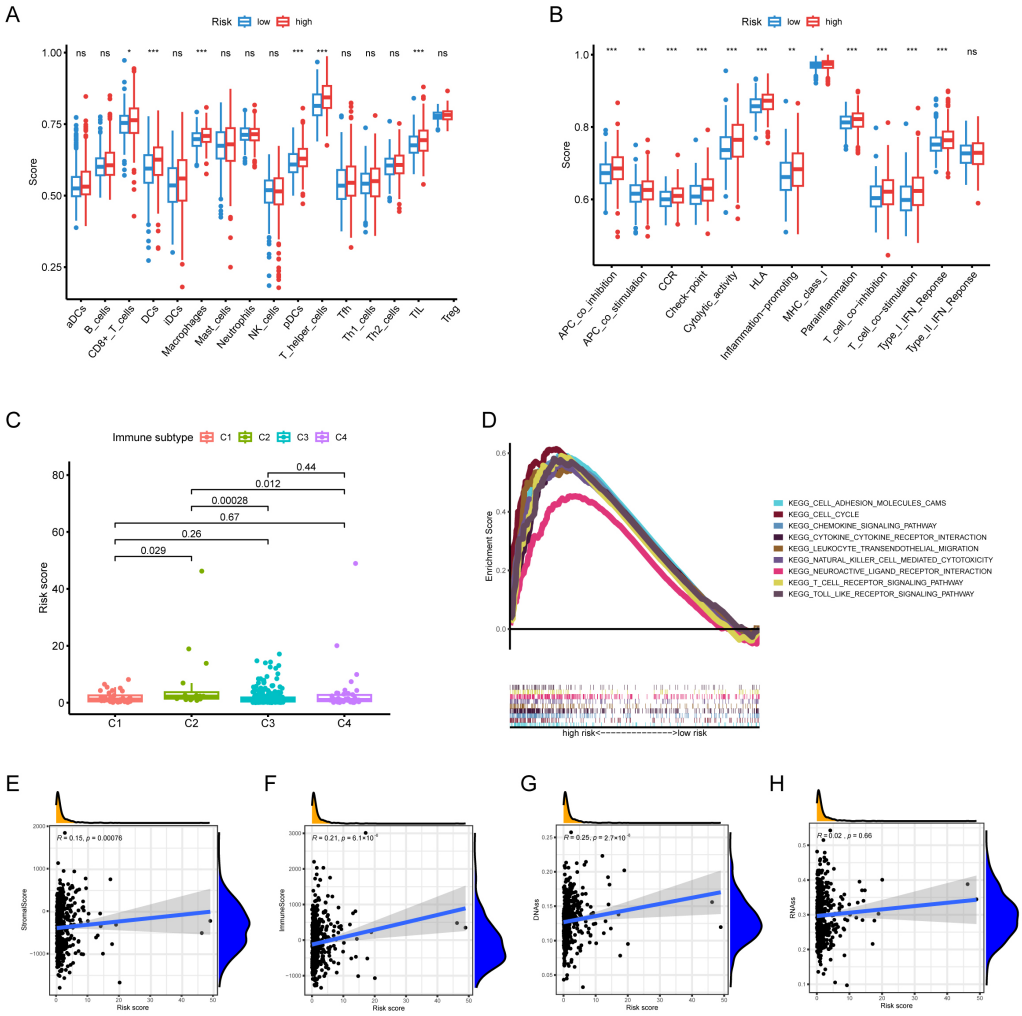

FIGURE 4. Correlation analysis between the risk score and immune infiltration status. (A) Comparison of immune cell subsets in low- and high-risk groups. (B) Comparison of immune function and pathways in the low- and high-risk groups. (C) Differences in immune classification among PCa patients with different risk scores. (D) Functional enrichment in risk groups revealed by GSEA analysis. (E) Scatterplot depicting the correlation between the stromal cell score. (F) Scatterplot depicting the correlation between the immune cell score. (G) Scatterplot depicting the correlation between DNAss. (H) Scatterplot depicting the correlation between RNAss. (*$p < 0.05$, **$p < 0.01$, ***$p < 0.001$). PCa: prostate cancer; GSEA: Gene Set Enrichment Analysis; DNAss: DNA methylation-based stemness scores; RNAss: RNA expression-based stemness scores.

of stromal cells ($p < 0.05$) as well as immune cell infiltration ($p < 0.05$) (Fig. 4E,F). Furthermore, we conducted a Spearman correlation analysis to investigate the association between the risk score and cancer stemness scores based on the stem cell score derived from DNA methylation (DNAss) and RNA sequencing (RNAss) (Fig. 4G,H). The findings demonstrate a statistically significant positive relationship between DNAss and the risk score ($p < 0.05$). Consequently, these results suggest a potential and significant correlation between the risk score of the prognostic model and the activity level of cancer stem cells, providing valuable insights into the role of cancer stemness in PCa.

3.5 The relationship between IRGs and drug sensitivity

We utilized the NCI-60 database, which comprises 60 distinct human cancer cell lines, to investigate the relationship between the expression levels of signature genes and the susceptibility of these cell lines to various drugs (Fig. 5). The study findings revealed a positive correlation between elevated levels of C3AR1 (Complement Component 3a Receptor 1), CLEC5A (C-Type Lectin Domain Family 5 Member A), OSM (Oncostatin M), SEMA4D (Semaphorin 4D) and SCARF1 (Scavenger Receptor Class F Member 1) and the sensitivity of cancer cells to several chemotherapeutic drugs, including Denileukin Diftitox Ontak, Artemether, ABT-199, Nelarabine, Methylprednisolone, Fluphenazine, Zalcitabine, Fludarabine and Ribavirin. Notably, the expression of SCARF1 demon-

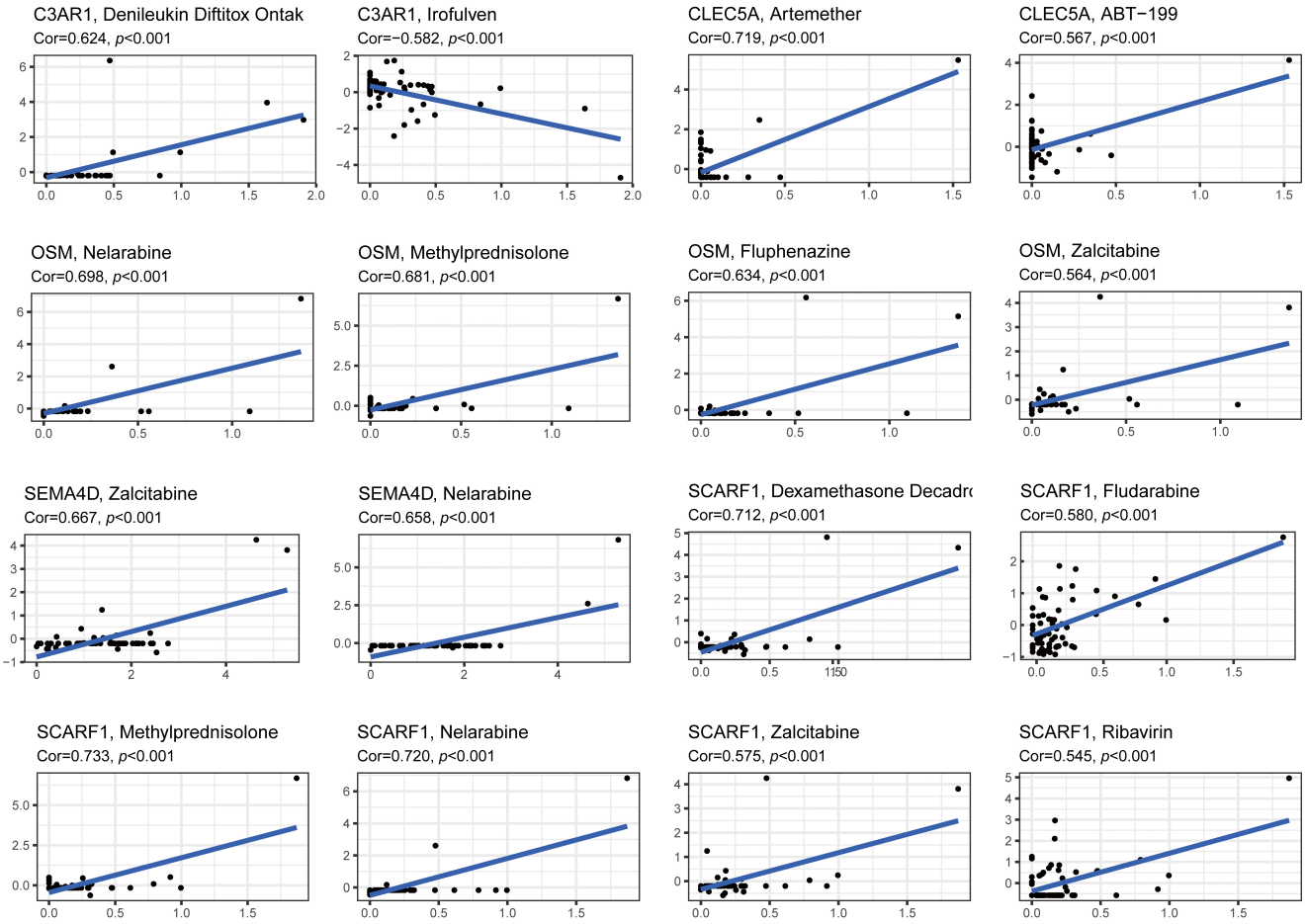

FIGURE 5. Investigation of gene-drug sensitivity using the cellminer database. In this figure, we explored gene-drug sensitivity utilizing the CellMiner database and identified the top 16 medications that exhibit the strongest connection with gene expression in an inflammatory-related prognostic model. Cor: correlation.

strated a positive association with the sensitivity of cancer cells to Denileukin Diftitox Ontak, Fludarabine, Methylprednisolone, Nelarabine, Zalcitabine, and Ribavirin. Conversely, the upregulation of C3AR1 was linked to increased resistance to Irofulven in cancer cells (Fig. 5). Table 3 shows the correlation analysis results, indicating significant associations with a p-value of < 0.001. These findings provide empirical evidence supporting the efficacy of the risk score in accurately predicting the responsiveness of cancer cells to these drugs, supporting the potential use of our proposed model in clinical settings to provide guidance in enhancing the precision of drug selection and treatment strategies.

4. Discussion

Despite recent advancements in our understanding of the biological behavior of PCa, it continues to be the predominant malignancy among males worldwide [28]. There is a growing recognition that the course of cancer in patients depends on a complex interplay between the tumor and the host's inflammatory response [29, 30]. Indeed, the involvement of inflammation in various other types of cancers has been well-established. Approximately 20% of human malignancies, such as those affecting the stomach, liver, and large intestine, are known to originate from chronic inflammation [16, 31–33]. Accumulating evidence suggests that a variety of inflammation mediators, including factors regulating the tumor microenvironment, activated transcriptional factors, pattern recognition receptors, cytokines and chemokines, play a significant role in the development, metastasis and prognosis of various human tumors, including PCa [34–37].

This study involved the development and validation of a novel prognostic model utilizing 17 inflammatory response genes, which exhibited a high degree of accuracy in predicting the prognosis of PCa patients. A nomogram was constructed using the identified IRGs within the TCGA cohort to estimate the 1-, 3- and 5-year overall survival rates for PCa patients. Notably, significant disparities in overall survival were observed between patients with high-risk scores and those with low-risk scores in both the training and validation datasets. Furthermore, both univariate and multivariate Cox regression analyses revealed that the risk score possessed independent prognostic significance, effectively predicting the survival outcomes of PCa patients. These findings underscore a robust association between the risk score and various clinicopathological characteristics, suggesting the potential of the risk score as a reliable prognostic tool for predicting the outcomes of PCa patients. Moreover, the study revealed a correlation between the risk

TABLE 3. Pearson correlation analysis between the expression of the 17 IRGs and chemotherapy drug sensitivity (shown are the 78 with $p < 0.001$).

Gene	Drugs	Cor	*p*.value
CARF1	Methylprednisolone	0.732640327	2.86×10^{-11}
SCARF1	Nelarabine	0.719889353	9.05×10^{-11}
CLEC5A	Artemether	0.718541463	1.02×10^{-10}
SCARF1	Dexamethasone Decadron	0.712263660	1.75×10^{-10}
OSM	Nelarabine	0.698284315	5.57×10^{-10}
OSM	Methylprednisolone	0.680533825	2.21×10^{-9}
SEMA4D	Zalcitabine	0.667448846	5.74×10^{-9}
SEMA4D	Nelarabine	0.658337585	1.09×10^{-8}
OSM	Fluphenazine	0.634060451	5.73×10^{-8}
C3AR1	Denileukin Diftitox Ontak	0.624168304	9.90×10^{-8}
C3AR1	Irofulven	−0.581910616	1.08×10^{-6}
SCARF1	Fludarabine	0.580322399	1.17×10^{-6}
SCARF1	Zalcitabine	0.574509681	1.59×10^{-6}
CLEC5A	ABT-199	0.566971598	2.32×10^{-6}
OSM	Zalcitabine	0.564243496	2.66×10^{-6}
SCARF1	Ribavirin	0.544935471	6.74×10^{-6}
C3AR1	Isotretinoin	0.544605132	6.85×10^{-6}
OSM	Pipobroman	0.537497963	9.50×10^{-6}
TNFRSF1B	Crizotinib	0.525435059	1.63×10^{-5}
C3AR1	Carmustine	0.525315019	1.64×10^{-5}
OSM	Ribavirin	0.512756781	2.81×10^{-5}
OSM	Thiotepa	0.49811976	5.12×10^{-5}
CLEC5A	Hydroxyurea	0.49686213	5.39×10^{-5}
OSM	Idarubicin	0.493478103	6.17×10^{-5}
C3AR1	Estramustine	0.492490569	6.41×10^{-5}
OSM	Triethylenemelamine	0.49035237	6.98×10^{-5}
OSM	Etoposide	0.486720695	8.04×10^{-5}
C3AR1	Fluphenazine	0.483938761	8.95×10^{-5}
SEMA4D	Ribavirin	0.482001356	9.64×10^{-5}
C3AR1	auranofin	0.481349531	9.88×10^{-5}
OSM	Dexamethasone Decadron	0.481275414	9.91×10^{-5}
C3AR1	Nelfinavir	0.479159675	0.000107422
SCN1B	Palbociclib	−0.479074824	0.000107768
OSM	DECITABINE	0.477732485	0.000113382
CLEC5A	Megestrol acetate	0.476523332	0.000118667
SEMA4D	Palbociclib	0.475939593	0.000121299
OSM	Chlorambucil	0.475426207	0.000123658
SCARF1	Fluphenazine	0.474493407	0.000128051
C3AR1	Megestrol acetate	0.474344406	0.000128766
OSM	Hydroxyurea	0.472306001	0.000138922

TABLE 3. Continued.

Gene	Drugs	Cor	*p*.value
CLEC5A	Cyclophosphamide	0.471781437	0.000141652
SEMA4D	Methylprednisolone	0.465587612	0.000177819
CLEC5A	Nandrolone phenpropionate	0.463489099	0.000191872
C3AR1	Artemether	0.461866301	0.000203429
OSM	Dexrazoxane	0.459815692	0.000218942
C3AR1	Alectinib	0.458489624	0.000229542
OPRK1	MONENSIN SODIUM	−0.45509378	0.000258858
DCBLD2	Artemether	−0.454977621	0.000259919
OSM	Teniposide	0.453464788	0.000274101
OSM	IDOXURIDINE	0.451903329	0.000289476
OSM	Valrubicin	0.45181132	0.000290406
OSM	Uracil mustard	0.450036076	0.000308892
SCARF1	Raltitrexed	0.448464457	0.000326147
C3AR1	rifa	0.447949184	0.000331992
SCARF1	Asparaginase	0.447314046	0.000339329
C3AR1	Lomustine	0.446607108	0.000347668
SCARF1	Hydroxyurea	0.446446673	0.000349586
TNFRSF1B	Artemether	0.444263098	0.000376672
OSM	Melphalan	0.443818735	0.000382412
OSM	BMN-673	0.442936265	0.000394049
SCARF1	Cytarabine	0.441758937	0.000410076
TNFRSF1B	LDK-378	0.44175406	0.000410143
SCARF1	Uracil mustard	0.435401571	0.000507321
KCNJ2	Pazopanib	−0.433546684	0.0005394
OSM	Nitrogen mustard	0.432191891	0.000563981
SEMA4D	Idarubicin	0.431698971	0.000573173
DCBLD2	auranofin	−0.430753758	0.000591181
SEMA4D	Hydroxyurea	0.427179062	0.000664016
SEMA4D	Asparaginase	0.422936188	0.000760949
SCARF1	Chlorambucil	0.421784927	0.00078937
OSM	M-AMSA	0.420448391	0.000823566
CLEC5A	auranofin	0.419580922	0.00084647
TNFRSF1B	ciclosporin	0.418882439	0.000865329
C3AR1	Dromostanolone Propionate	0.417659117	0.000899275
SEMA4D	Dexrazoxane	0.416885111	0.000921368
CLEC5A	Masoprocol	0.41630485	0.000938252
OSM	Cytarabine	0.415985959	0.000947648
C3AR1	Cyclophosphamide	0.415764105	0.000954236

IRGs: inflammatory-related genes; Cor: correlation.

score of IRGs and the tumor's immunological status, further highlighting the potential clinical relevance of this prognostic model in PCa immunotherapy. Lastly, it was demonstrated that the expression levels of the prognostic genes were significantly correlated with the sensitivity of chemotherapeutic agents, emphasizing the utility of this model in aiding the selection of optimal treatment strategies for PCa patients.

The TME has gained widespread recognition for its close association with various processes such as tumor cell proliferation, survival, invasion and metastasis [38]. In this context, the inflammatory response plays a crucial role in the systemic immune response, serving as a critical mechanism for the early recruitment of inflammatory factors and the establishment of the tumor microenvironment [39]. In addition to stimulating the immune system and contributing to the inflammatory response, inflammatory response-related genes also play a role in shaping the TME [40]. PCa is often characterized as a "cold" tumor due to its immunosuppressive microenvironment [41–44]. TILs have been implicated in the progression of PCa by inhibiting the activity of T-effector cells [45]. The present study revealed a significant positive correlation between the risk score of IRGs and the abundance of immune infiltrating cells. Thus, our present research findings suggest that the IRGs included in the model could potentially serve as valuable tools for guiding immunotherapy in PCa patients.

Although the risk score of IRGs has shown potential in predicting the immunological status and prognosis of PCa patients, our study had some limitations. The therapeutic usefulness of this predictive model should be verified by prospective research, as it was created and validated using retrospective data from the TCGA and cBioPortal public databases. The therapeutic applicability of this predictive model should be confirmed through prospective studies, as it was developed and validated using retrospective data from the TCGA and cBioPortal public databases. In our future work, we plan to conduct experimental validation, both *in vitro* and *in vivo*, potentially extending our investigations to clinical samples. Moreover, exploring the underlying molecular mechanisms is another avenue requiring further examination.

5. Conclusions

Examining the prognostic implications of inflammatory-related factors in PCa patients is a significant and innovative approach. In this present study, we developed a predictive signature comprising 17 IRGs associated with inflammation, which demonstrated high accuracy in predicting the survival outcomes of PCa patients, as validated in both the training dataset (TCGA) and the validation dataset (cBioPortal). Collectively, these IRGs hold potential as valuable biomarkers and therapeutic targets for individuals diagnosed with PCa, offering a promising avenue for further scientific investigation.

AVAILABILITY OF DATA AND MATERIALS

The study incorporates the primary data within the article. Further inquiries can be directed to the corresponding authors.

AUTHOR CONTRIBUTIONS

ZYH—study design and administration, writing editing; MW and HD—extraction data; MW—analysis and interpretation of data & writing original draft; All the authors were involved in the study. All the authors took part in the discussions of the results and contributed to the manuscript.

ETHICS APPROVAL AND CONSENT TO PARTICIPATE

Not applicable.

ACKNOWLEDGMENT

This work was supported by National Key Clinical Specialties Construction Program. We would like to extend our heartfelt gratitude to the TCGA and cBioPortal databases for generously offering accessible data and the R software for unrestricted utilization without charge.

FUNDING

This research received no external funding.

CONFLICT OF INTEREST

The authors declare no conflict of interest.

REFERENCES

[1] Khan MM, Sharma V, Serajuddin M. Emerging role of miRNA in prostate cancer: a future era of diagnostic and therapeutics. Gene. 2023; 888: 147761.

[2] Cooperberg MR, Cowan J, Broering JM, Carroll PR. High-risk prostate cancer in the United States, 1990–2007. World Journal of Urology. 2008; 26: 211–218.

[3] D'Amico AV, Whittington R, Malkowicz SB, Schultz D, Blank K, Broderick GA, *et al*. Biochemical outcome after radical prostatectomy, external beam radiation therapy, or interstitial radiation therapy for clinically localized prostate cancer. JAMA. 1998; 280: 969–974.

[4] Wang J, Xia HH, Zhang Y, Zhang L. Trends in treatments for prostate cancer in the United States, 2010–2015. American Journal of Cancer Research. 2021; 11: 2351–2368.

[5] Mahal BA, Butler S, Franco I, Spratt DE, Rebbeck TR, D'Amico AV, *et al*. Use of active surveillance or watchful waiting for low-risk prostate cancer and management trends across risk groups in the United States, 2010–2015. JAMA. 2019; 321: 704–706.

[6] Burgess L, Roy S, Morgan S, Malone S. A review on the current treatment paradigm in high-risk prostate cancer. Cancers. 2021; 13: 4257.

[7] Mano R, Eastham J, Yossepowitch O. The very-high-risk prostate cancer: a contemporary update. Prostate Cancer and Prostatic Diseases. 2016; 19: 340–348.

[8] Mossanen M, Krasnow RE, Nguyen PL, Trinh QD, Preston M, Kibel AS. Approach to the patient with high-risk prostate cancer. Urologic Clinics of North America. 2017; 44: 635–645.

[9] Adamaki M, Zoumpourlis V. Prostate cancer biomarkers: from diagnosis to prognosis and precision-guided therapeutics. Pharmacology & Therapeutics. 2021; 228: 107932.

[10] Chung BH. The role of radical prostatectomy in high-risk prostate cancer. Prostate International. 2013; 1: 95–101.

[11] Costello AJ. Considering the role of radical prostatectomy in 21st century prostate cancer care. Nature Reviews Urology. 2020; 17: 177–188.

[12] Pérez-Gómez JM, Montero-Hidalgo AJ, Fuentes-Fayos AC, Sarmento-Cabral A, Guzmán-Ruiz R, Malagón MM, *et al*. Exploring the role of the inflammasomes on prostate cancer: interplay with obesity. Reviews in Endocrine and Metabolic Disorders. 2023; 24: 1165–1187.

[13] Cai T, Santi R, Tamanini I, Galli IC, Perletti G, Bjerklund Johansen TE, *et al*. Current knowledge of the potential links between inflammation and prostate cancer. International Journal of Molecular Sciences. 2019; 20: 3833.

[14] Zhang L, Wang Y, Qin Z, Gao X, Xing Q, Li R, *et al*. Correlation between prostatitis, benign prostatic hyperplasia and prostate cancer: a systematic review and meta-analysis. Journal of Cancer. 2020; 11: 177–189.

[15] Murata M. Inflammation and cancer. Environmental Health and Preventive Medicine. 2018; 23: 50.

[16] Zhao H, Wu L, Yan G, Chen Y, Zhou M, Wu Y, *et al*. Inflammation and tumor progression: signaling pathways and targeted intervention. Signal Transduction and Targeted Therapy. 2021; 6: 263.

[17] Catalano M, Roviello G, Santi R, Villari D, Spatafora P, Galli IC, *et al*. Inflammation in urological malignancies: the silent killer. International Journal of Molecular Sciences. 2023; 24: 866.

[18] Kustrimovic N, Bombelli R, Baci D, Mortara L. Microbiome and prostate cancer: a novel target for prevention and treatment. International Journal of Molecular Sciences. 2023; 24: 1511.

[19] McAllister M, Constâncio V, Patek S, Gan HWG, Bailey P, Wheadon H, *et al*. Inflammatory infiltration is associated with AR expression and poor prognosis in hormone naive prostate cancer. The Prostate. 2020; 80: 1353–1364.

[20] Thapa D, Ghosh R. Chronic inflammatory mediators enhance prostate cancer development and progression. Biochemical Pharmacology. 2015; 94: 53–62.

[21] Cerami E, Gao J, Dogrusoz U, Gross BE, Sumer SO, Aksoy BA, *et al*. The cBio cancer genomics portal: an open platform for exploring multidimensional cancer genomics data. Cancer Discovery. 2012; 2: 401–404.

[22] Gao J, Aksoy BA, Dogrusoz U, Dresdner G, Gross B, Sumer SO, *et al*. Integrative analysis of complex cancer genomics and clinical profiles using the cBioPortal. Science Signaling. 2013; 6: pl1.

[23] Subramanian A, Tamayo P, Mootha VK, Mukherjee S, Ebert BL, Gillette MA, *et al*. Gene set enrichment analysis: a knowledge-based approach for interpreting genome-wide expression profiles. Proceedings of the National Academy of Sciences. 2005; 102: 15545–15550.

[24] Hänzelmann S, Castelo R, Guinney J. GSVA: gene set variation analysis for microarray and RNA-Seq data. BMC Bioinformatics. 2013; 14: 7.

[25] Xiong X, Chen C, Li X, Yang J, Zhang W, Wang X, *et al*. Identification of a novel defined inflammation-related long noncoding RNA signature contributes to predicting prognosis and distinction between the cold and hot tumors in bladder cancer. Frontiers in Oncology. 2023; 13: 972558.

[26] Yoshihara K, Shahmoradgoli M, Martínez E, Vegesna R, Kim H, Torres-Garcia W, *et al*. Inferring tumour purity and stromal and immune cell admixture from expression data. Nature Communications. 2013; 4: 2612.

[27] Shankavaram UT, Varma S, Kane D, Sunshine M, Chary KK, Reinhold WC, *et al*. CellMiner: a relational database and query tool for the NCI-60 cancer cell lines. BMC Genomics. 2009; 10: 277.

[28] Berenguer CV, Pereira F, Câmara JS, Pereira JAM. Underlying features of prostate cancer-statistics, risk factors, and emerging methods for its diagnosis. Current Oncology. 2023; 30: 2300–2321.

[29] Fan L, Wang R, Chi C, Cai W, Zhang Y, Qian H, *et al*. Systemic immune-inflammation index predicts the combined clinical outcome after sequential therapy with abiraterone and docetaxel for metastatic castration-resistant prostate cancer patients. The Prostate. 2018; 78: 250–256.

[30] McArdle PA, Mir K, Almushatat ASK, Wallace AM, Underwood MA, McMillan DC. Systemic inflammatory response, prostate-specific antigen and survival in patients with metastatic prostate cancer. Urologia Internationalis. 2006; 77: 127–129.

[31] Greten FR, Grivennikov SI. Inflammation and cancer: triggers, mechanisms, and consequences. Immunity. 2019; 51: 27–41.

[32] Sfanos KS, De Marzo AM. Prostate cancer and inflammation: the evidence. Histopathology. 2012; 60: 199–215.

[33] Stark T, Livas L, Kyprianou N. Inflammation in prostate cancer progression and therapeutic targeting. Translational Andrology and Urology. 2015; 4: 455–463.

[34] Haverkamp J, Charbonneau B, Ratliff TL. Prostate inflammation and its potential impact on prostate cancer: a current review. Journal of Cellular Biochemistry. 2008; 103: 1344–1353.

[35] Lan T, Chen L, Wei X. Inflammatory cytokines in cancer: comprehensive understanding and clinical progress in gene therapy. Cells. 2021; 10: 100.

[36] Pandey S, Singh S, Anang V, Bhatt AN, Natarajan K, Dwarakanath BS. Pattern recognition receptors in cancer progression and metastasis. Cancer Growth and Metastasis. 2015; 8: 25–34.

[37] Chen L, Deng H, Cui H, Fang J, Zuo Z, Deng J, *et al*. Inflammatory responses and inflammation-associated diseases in organs. Oncotarget. 2018; 9: 7204–7218.

[38] Baxevanis CN, Fortis SP, Perez SA. The balance between breast cancer and the immune system: challenges for prognosis and clinical benefit from immunotherapies. Seminars in Cancer Biology. 2021; 72: 76–89.

[39] Bonavita E, Bromley CP, Jonsson G, Pelly VS, Sahoo S, Walwyn-Brown K, *et al*. Antagonistic inflammatory phenotypes dictate tumor fate and response to immune checkpoint blockade. Immunity. 2020; 53: 1215–1229.e18.

[40] Zheng H, Luo W, Li Y, Peng G, Zhou D, Tang D, *et al*. Identification and development of inflammatory response-related genes signature associated with prognosis evaluation and immune status of bladder cancer. Frontiers in Cell and Developmental Biology. 2022; 10: 837849.

[41] Fay EK, Graff JN. Immunotherapy in prostate cancer. Cancers. 2020; 12: 1752.

[42] Di Lorenzo G, Buonerba C, Kantoff PW. Immunotherapy for the treatment of prostate cancer. Nature Reviews Clinical Oncology. 2011; 8: 551–561.

[43] Sooi K, Walsh R, Kumarakulasinghe N, Wong A, Ngoi N. A review of strategies to overcome immune resistance in the treatment of advanced prostate cancer. Cancer Drug Resistance. 2023; 6: 656–673.

[44] Séguier D, Adams ES, Kotamarti S, D'Anniballe V, Michael ZD, Deivasigamani S, *et al*. Intratumoural immunotherapy plus focal thermal ablation for localized prostate cancer. To be published in Nature Reviews Urology. 2023. [Preprint].

[45] Cha HR, Lee JH, Ponnazhagan S. Revisiting immunotherapy: a focus on prostate cancer. Cancer Research. 2020; 80: 1615–1623.

How to cite this article: Mao Wang, Hao Dong, Zhi-Yao He. A novel prognosis and drug-susceptibility predictor based inflammatory-related genes signature in prostate cancer. Journal of Men's Health. 2024; 20(7): 26-38. doi: 10.22514/jomh.2024.107.